Available online at www.sciencedirect.com

SCIENCE DIRECT

Experimental Neurology 195 (2005) 458 – 474

Experimental Neurology

www.elsevier.com/locate/yexnr

Regular Article

Heterogeneity among hippocampal pyramidal neurons revealed by their relation to theta-band oscillation and synchrony

Brian H. Bland[a,*], Jan Konopacki[b], Richard Dyck[a]

[a]*Department of Psychology, Behavioral Neuroscience Research Group, University of Calgary, 2500 University Dr. NW, Calgary, Alberta, Canada T2N 1N4*

[b]*Department of Neurobiology, University of Lodz, Poland*

Received 11 April 2005; revised 17 May 2005; accepted 10 June 2005
Available online 14 July 2005

Abstract

Intracellular recordings were made in the dorsal hippocampal formation of urethane-anesthetized rats as the local field activity spontaneously cycled between a synchronous condition termed theta and an asynchronous condition termed LIA. All cells reported in this study were labeled with Neurobiotin and classified as theta-related or non-theta-related according to the system of Colom and Bland [Colom, L.V., Bland, B.H., 1987. State-dependent spike train dynamics of hippocampal formation neurons: evidence for theta-ON and theta-OFF cells. Brain Res. 422; 277-286]. The findings are the first demonstration that hippocampal pyramidal cells are functionally heterogeneous in relation to the generation of theta-band oscillation and synchrony. In field CA1 pyramidal cells formed theta-related subsets of phasic theta-ON cells and tonic theta-ON cells and non-theta-related subsets of simple spike discharging cells, complex spike discharging cells and "silent" cells. Similar findings were evident for CA3 pyramidal cells.

Keywords: Intracellular; Labeling; CA1; CA3; Neurobiotin

Introduction

Theta-band oscillation and synchrony generated in the hippocampus and related limbic structures of mammals are recorded as an extracellular field potential consisting of a sinusoidal-like waveform with an amplitude $\leq$2 mV and a narrowband frequency range of 3–12 Hz. The asynchronous field activity of the same structures, termed large amplitude irregular activity (LIA), is an irregular waveform with a broadband frequency range of 0.5–25 Hz (Leung et al., 1982). Brain rhythms may function to entrain large neural networks into selective modes of information processing related to perceptual and behavioral states. The neural networks underlying theta-band oscillation and synchrony are comprised largely of the ascending brainstem hippocampal synchronizing pathways (Bland and Oddie, 1998; Vertes and Kocsis, 1997) while its functional significance lies in providing voluntary motor systems with continually updated feedback on their performance relative to changing environmental (sensory) conditions (sensorimotor integration) (Bland and Oddie, 2001). Much research in recent years has been directed at studying the discharge properties of cells in the hippocampal formation and associated limbic structures, related to the field states of theta and LIA (Bland et al., 2002, Vertes et al., 2004). Theta-related cells comprise two basic populations, termed theta-ON and theta-OFF (Colom and Bland, 1987). These cell classes have been documented in nuclei from the lower brainstem through to the cerebral cortex, representing a general organization of cellular interactions involved in the generation of theta-band oscillation and synchrony (Bland, 2000). Participation in the generation of theta-band oscillation and synchrony by theta-ON and theta-OFF cells involves a combination of extrinsic inputs interacting with intrinsic membrane properties (Bland and Colom, 1993; Bland et al., 2002; Buzsaki, 2002). The anatomical identity of theta-related cell populations is thus crucial to the

* Corresponding author.
E-mail address: bhbland@ucalgary.ca (B.H. Bland).

0014-4886/$ - see front matter © 2005 Elsevier Inc. All rights reserved.
doi:10.1016/j.expneurol.2005.06.007

understanding of these cellular interactions. In particular, there has been controversy associated with the role of hippocampal pyramidal cells in the generation of theta-band oscillation and synchrony. Bland and Colom (1993) proposed that despite their anatomical similarity, pyramidal cells form functionally different subsets, for example, some related to theta generation and sensorimotor integration and others related to spatial processing. The focus of the present work was to characterize anatomically identified CA1 and CA3 pyramidal cells in relation to the generation of hippocampal field activity. Intracellular recordings were made in the dorsal hippocampus of urethane-anesthetized rats as local field activity spontaneously cycled between theta and LIA. All cells reported in the present study were successfully labeled with Neurobiotin and classified as theta-related or non-related, according to the system of Colom and Bland (1987).

Materials and methods

Subjects and surgical procedures

The data were obtained from 67 male Long Evans black-hooded rats (125 to 130 g) supplied by the Life and Environmental Sciences Animal Care Facility at the University of Calgary. The rats were initially anesthetized with halothane while tracheal and jugular cannulae were inserted. Halothane was then discontinued and urethane was administered via the jugular cannula to maintain an appropriate level of anesthesia during the remaining surgical and experimental procedures. The rats were placed in the stereotaxic instrument with the plane between bregma and lambda leveled to horizontal. Body temperature was maintained at 37°C and heart rate was monitored constantly throughout the experiment. An uninsulated tungsten wire placed in the cortex, anterior to bregma, served as the indifferent electrode and the stereotaxic frame was connected to ground. A tungsten microelectrode (0.2–0.5 MΩ) for recording hippocampal (HPC) field activity was placed in the right dorsal hippocampal formation either in the dentate molecular layer (3.0–3.3 mm posterior to bregma, 2.0–2.5 mm lateral to the midline and 2.4–2.8 mm ventral to the dural surface) or in stratum oriens (3.0–3.3 mm posterior to bregma, 2.0–2.5 mm lateral to the midline and 1.8–2.0 mm ventral to the dural surface). Intracellular recordings of CA1 pyramidal cells in the left HPC were made at the same posterior and lateral coordinates, starting at the alvear surface and continuing ventral to the lower (endal) blade of the dentate granule cells. Intracellular recordings in CA3 were made at the same posterior coordinates, 3.6 mm lateral to the midline and starting 2.0 mm ventral to dural surface. Details of the procedures for preparing the site for intracellular recordings have been described previously (Bland and Konopacki, 2000; Bland et al., 2002; Konopacki et al., 2003).

Electrophysiological recordings

Intracellular recordings in HPC cells were made with glass microelectrodes (80–120 MΩ) filled with 2 M potassium acetate and 2% Neurobiotin (Vector Laboratories). Details of these procedures have been published previously (Bland and Konopacki, 2000; Konopacki et al., 1992, 2003). Signals were lead through an active bridge circuit (Axon Instruments, Axoclamp 2A) allowing simultaneous injection of current and measurement of membrane potential (Vm). The bridge balance was monitored and adjusted as necessary throughout the recording procedures. These and all other signals were displayed on a digital oscilloscope (Tektronix TDS 420) and stored on an FM tape recorder (Teac XR-30) for subsequent off-line data analysis. Once a recording was considered stabilized (defined as the absence of applied hyperpolarizing DC current and a stable membrane potential of at least −55 mV for 5 min), the experimental protocol was initiated. First, recordings were taken during the spontaneously occurring HPC field activities of synchrony (theta) and asynchrony (LIA), ensuring a minimum duration of 1 min of each type was accumulated. Following completion of this part of the protocol, a series of short duration hyperpolarizing current pulses (100 ms duration, −100, −200, −300 and −400 pA) and depolarizing current pulses (100, 200, 300 and 400 pA) were administered in ascending magnitude, respectively, for purposes of carrying out standard electrophysiological measurements. Cells were numbered sequentially in the intracellular protocol we began several years ago. The protocol for intracellular staining was modified slightly from the procedures previously described (Kita and Armstrong, 1991). Positive pulses were applied (5 nA, 2 Hz, 100 ms duration) for 1 to 10 min and the electrode was left inside the cell for 2 to 3 min before it was withdrawn.

Data analysis

Data were analyzed using the Axon Instruments Axoscope 8.2, Microcal Origin 4.1, and DataWave 6.1 software. Spike height and duration were determined from the first action potential evoked at threshold levels of depolarization. Resting membrane potentials were defined as an average of a series of a minimum of 30 membrane potentials measured between the spike discharges occurring during the LIA field conditions. Input resistance was provided as the slope of the linear regression line fitted through the linear portion of the current–voltage plots derived from the family of hyperpolarizing and depolarizing current pulse injections. MPOs, defined as the slow intracellular membrane potential oscillations occurring at extracellular theta frequencies, were measured at the positive and negative peaks (see Bland et al., 2002) using the cursor facility in the Axoscope 8 program, and calculated as the statistical average of a minimum of 50 to 60 individual MPOs measured in each experimental condition. Additional data analyses included:

(1) fast Fourier transforms of the field activities and membrane potential oscillations (intracellular membrane potentials filtered narrow band, 1 Hz–10 Hz) of theta and LIA, (2) autocorrelation histograms of the spike trains during theta and LIA, (3) cross-correlations between MPOs and theta field activity and (4) quantification and statistical analysis using *t* tests of the spike discharges occurring during each experimental condition.

Imaging techniques and cellular identification

At the termination of a recording session, all animals were administered an overdose of sodium pentobarbital and perfused transcardially with 50 ml phosphate-buffered saline (PBS, 0.1M, pH 7.4) followed by 300 ml of 4% paraformaldehyde in PBS. The brain was removed and immersed in the fixative for an additional 4 h and then cryoprotected, overnight, in a solution of 30% sucrose in PBS. The brains were frozen and coronal sections were cut at 50 μm on a sliding microtome. Every section through the hippocampal formation was collected in PBS and then incubated for 2 h in a 1:500 solution of avidin–HRP in PBS. After 3 washes in PBS, the neurobiotin–avidin–HRP complex was visualized by incubating the sections in a chromogen solution consisting of 10 ml 0.1 M Tris-buffered saline containing 5 mg diaminobenzidine, 40 μg nickel ammonium sulfate and 10 μl 30% hydrogen peroxide. When the reaction was complete, the sections were washed 3 times in PBS and then mounted onto gelatin-coated glass slides and allowed to dry. The sections were dehydrated in an ascending series of ethanol, cleared in xylene and cover slipped using Permount. The labeled cells were identified using a Zeiss Axioplan 2 microscope at 20× and digital images were captured and serially reconstructed using Openlab (v. 3.0, Improvision) and Adobe Photoshop (v. 6.0, Adobe Corp.) running on an Apple G4.

Results

Theta- and non-theta-related categories of identified CA1 pyramidal cells

A total of 20 CA1 pyramidal cells were successfully recorded and as a result of multiple fills, 25 CA1 pyramidal cells were labeled. These cells were classified according to the system of Colom and Bland (1987) as phasic theta-ON ($n = 9$), tonic theta-ON ($n = 2$) and non-related ($n = 9$). Non-related CA1 pyramidal cells were either of the discharging type ($n = 3$) or totally silent during theta and LIA ($n = 6$). The theta frequency range during all experiments was 3.2–4 Hz. Data for all CA1 pyramidal cells are presented in Table 1.

CA1 pyramidal phasic theta-ON cells

Nine of 20 CA1 pyramidal cells were classified as phasic theta-ON cells. Two recordings resulted in the labeling of two pyramidal cells and one recording resulted in the labeling of three pyramidal cells. Fig. 1 shows a representative example of one of these cell recordings (cell 256) during the spontaneous occurrence of either hippocampal

Table 1
CA1 pyramidal cell summary

Cell type and number	Cell class	Input resistance (MΩ)	Average membrane potential (mV)	Spike height (mV)	Average MPO amplitude (theta only) (mV)	Discharge rate—theta (mean ± SE)	Discharge rate—LIA (mean ± SE)
CA1 Pyr (248)	Phasic ON	31	60	52	6.8	6.1 ± 0.4*	4.4 ± 0.4
CA1 Pyr (256)	Phasic ON	29	62	60	9.2	12.1 ± 0.5*	2.8 ± 0.5
CA1 Pyr (259)	Phasic ON	32	60	60	9.1	10.0 ± 1.2*	4.3 ± 0.8
CA1 Pyr (260)	Phasic ON	27	60	55	9.1	5.9 ± 0.3*	3.0 ± 0.5
CA1 Pyr (266)	Phasic ON	30	60	54	5.2	7.2 ± 0.6*	5.0 ± 0.2
CA1 Pyr (268)	Phasic ON	25	65	63	8.0	7.2 ± 0.3*	4.6 ± 0.5
CA1 Pyr (277)	Phasic ON	29	59	72	9.8	5.0 ± 0.2*	3.3 ± 0.4
CA1 Pyr (280)	Phasic ON	26	63	67	12.6	11.2 ± 0.9*	3.4 ± 0.5
CA1 Pyr (306)	Phasic ON	28	64	68	7.9	9.7 ± 0.4*	3.9 ± 0.9
CA1 Pyr (267)	Tonic ON	27	67	62	–	6.8 ± 0.3*	5.0 ± 0.4
CA1 Pyr (289)	Tonic ON	26	61	55	–	11.7 ± 0.4*	5.8 ± 0.8
CA1 Pyr (252)	Silent	28	60	55	–	–	–
CA1 Pyr (258)	Silent	31	60	65	–	–	–
CA1 Pyr (270)	Silent	25	65	55	–	–	–
CA1 Pyr (272)	Discharging	29	60	50	–	5.5 ± 0.3	4.1 ± 0.7
CA1 Pyr (281)	Silent	27	65	60	–	–	–
CA1 Pyr (282)	Discharging	30	58	60	–	4.3 ± 0.4	4.0 ± 0.4
CA1 Pyr (291)	Complex	26	62	60	–	0.8 ± 0.1	1.1 ± 0.3
CA1 Pyr (292)	Silent	31	70	60	–	–	–
CA1 Pyr (296)	Silent	30	64	60	–	–	–

Asterisk indicates significant differences at $P < 0.05$.

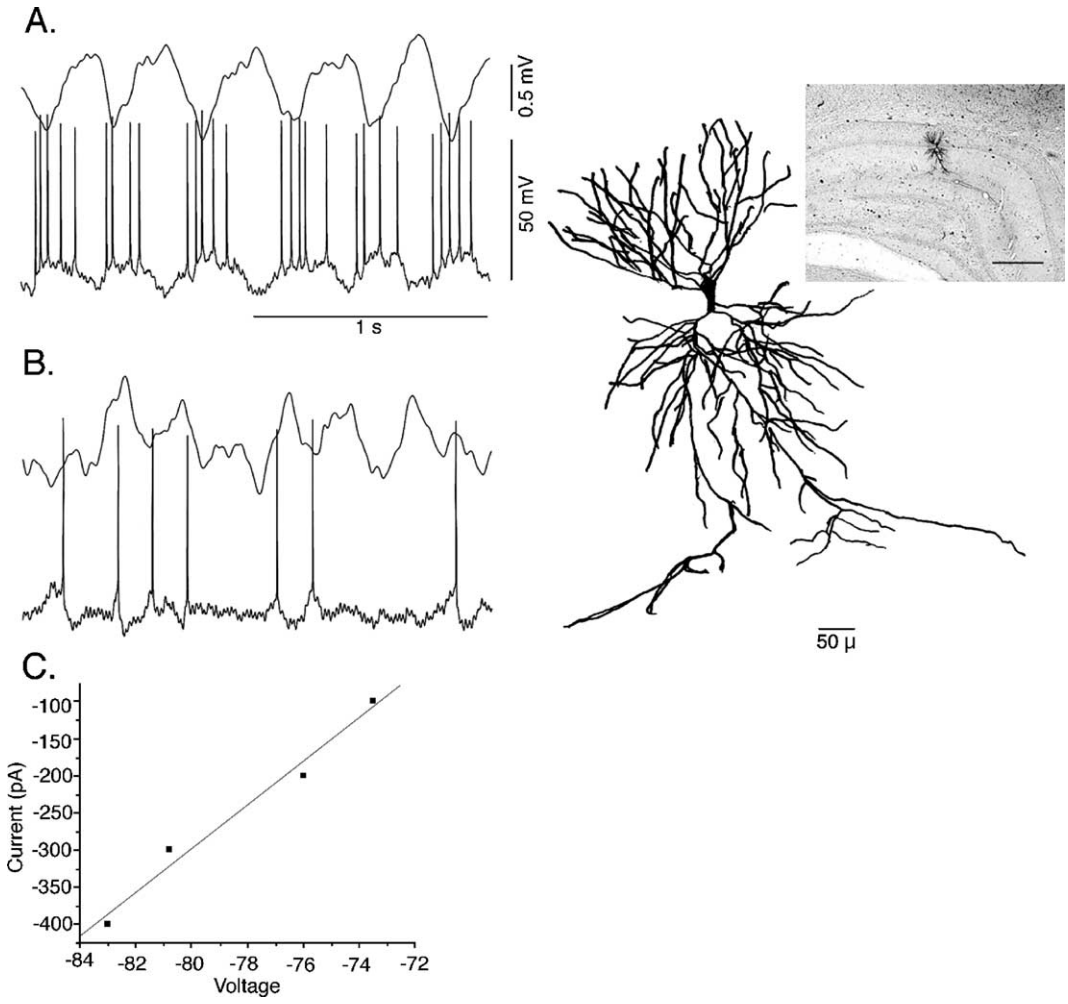

Fig. 1. (A) Relationship between spontaneously occurring hippocampal theta field activity and discharges of a CA1 pyramidal cell. Top: the hippocampal field activity recorded dorsal to the CA1 pyramidal cell layer in stratum oriens; bottom: the discharge pattern of a CA1 pyramidal cell (256) classified as a phasic theta-ON cell (positivity up in all traces). The cell discharged in a rhythmic pattern with 4–5 spikes riding on the positive phase of the MPOs and the negative phase of the locally recorded extracellular theta field. (B) Relationship of the same cell to spontaneously occurring hippocampal LIA field activity. Note the overall lower discharge rate, irregular discharge pattern and lack of MPOs. (C) Current–voltage plot of cell 256, input resistance = 29 MΩ. Low power photomicrograph insert shows the location of the cell in the CA1 pyramidal layer while the higher power magnification insert confirmed its identity as a CA1 pyramidal cell. Scale bar = 50 µ.

theta (Fig. 1A) or LIA (Fig. 1B). During theta field activity, the cell membrane potential underwent a depolarizing shift of 5–10 mV and discharged 4–5 spikes (mean discharge rate = 12.08 ± 0.53 Hz) on the positive peak of well developed intracellular MPOs (mean amplitude = 9.2 ± 0.5 mV) and on the negative peak of the theta field activity (mean frequency = 3.2 Hz) recorded in the stratum oriens. During LIA, MPOs were absent and the cell discharged in an irregular, non-rhythmic pattern and an overall lower discharge rate (mean discharge rate = 2.84 ± 0.46 Hz) significantly different from the discharge rate during theta field activity (t = 17.32, P = 7.426, $P < 0.05$). Fig. 1C presents the current–voltage plot along with the linear regression curve (input resistance = 29 mΩ). The injection of Neurobiotin into cell 256 resulted in the labeling of one cell, shown in the low power photomicrograph insert to be located in the CA1 pyramidal layer and the higher magnification insert revealing its identity as a CA1 pyramidal cell. Fig. 2 presents the analyses carried out on cell 256 from Fig. 1. Left-side panels show analyses for the theta field conditions and right-side panels show the equivalent analyses for the LIA field conditions. The upper left panel is the FFT calculated for the extracellular theta field (mean frequency = 3.2 Hz), the middle left panel the FFT calculated for the MPOs (mean frequency = 3.2 Hz) and the lower left panel the autocorrelation histogram of the spike train, indicating a rhythmic discharge pattern. The upper right panel is the FFT calculated for the LIA field condition (theta peak absent), the middle right panel the FFT calculated for the MPOs (theta peak absent) and the lower right panel is the autocorrelation histogram of the spike train, indicating an irregular, non-rhythmic discharge pattern and a lower discharge rate compared to that occurring during the LIA field condition. Fig. 3 shows a representative

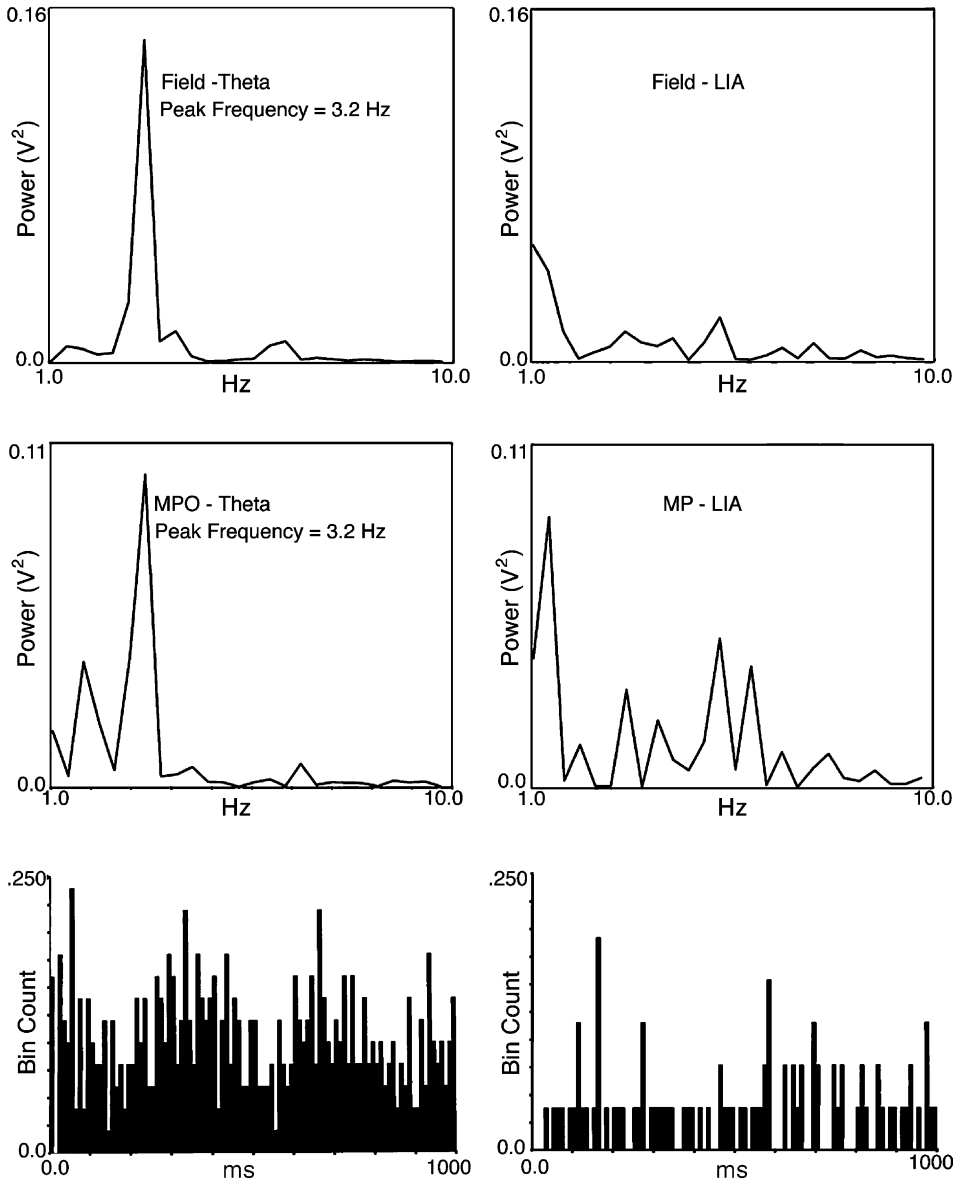

Fig. 2. Detailed analyses of the extracellular fields, intracellular membrane potentials and spike discharges of phasic theta-ON cell 256 during theta field activity (left-side panels) and LIA (right-side panels). Fast Fourier analysis of extracellular theta field activity (top left panel), fast Fourier analysis of MPOs during theta field activity (middle left panel) and autocorrelation histogram of rhythmic spike discharges during theta field activity (bottom left panel). Fast Fourier analysis of extracellular LIA field activity (top right panel), fast Fourier analysis of MPOs during theta field activity (middle right panel) and autocorrelation histogram of irregular spike discharges during LIA field activity (bottom right panel).

example (phasic theta-ON cell 306) of the depolarizing shift in the membrane potential (in this example 7.2 mV) that occurred at the transition from LIA to theta field activity.

CA1 pyramidal tonic theta-ON cells

Two out of 20 CA1 pyramidal cells were classified as tonic theta-ON cells. Fig. 4 shows an example of one of these cell recordings (cell 289) during the spontaneous occurrence of either HPC theta (Fig. 4A) or LIA (Fig. 4B). During theta field activity (mean frequency = 3.2 Hz), the cell increased its discharge rate in a simple spike irregular pattern (mean discharge rate = 11.7 ± 0.36 Hz) and MPOs were absent. During LIA, MPOs were absent and the cell fired in the same discharge pattern, but at a significantly lower rate (mean discharge rate = 5.8 ± 0.79 Hz) (t = 3.5907, P = 0.00209, $P < 0.05$). The injection of Neurobiotin into cell 289 resulted in the labeling of one cell, shown in the low power photomicrograph insert to be located in the CA1 pyramidal layer and the higher magnification insert revealing its identity as a CA1 pyramidal cell. Fig. 5 presents the analyses carried out on cell 289 from Fig. 4. Left-side panels show analyses for the theta field conditions and right-side panels show the

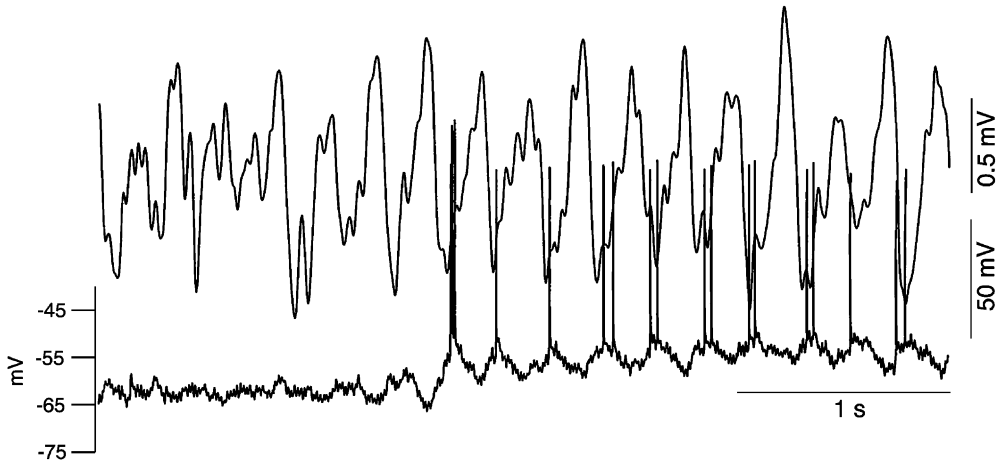

Fig. 3. A representative example (phasic theta-ON cell 306) of the depolarizing shift in the membrane potential (in this example 7.2 mV) that occurs at the transition from LIA to theta field activity.

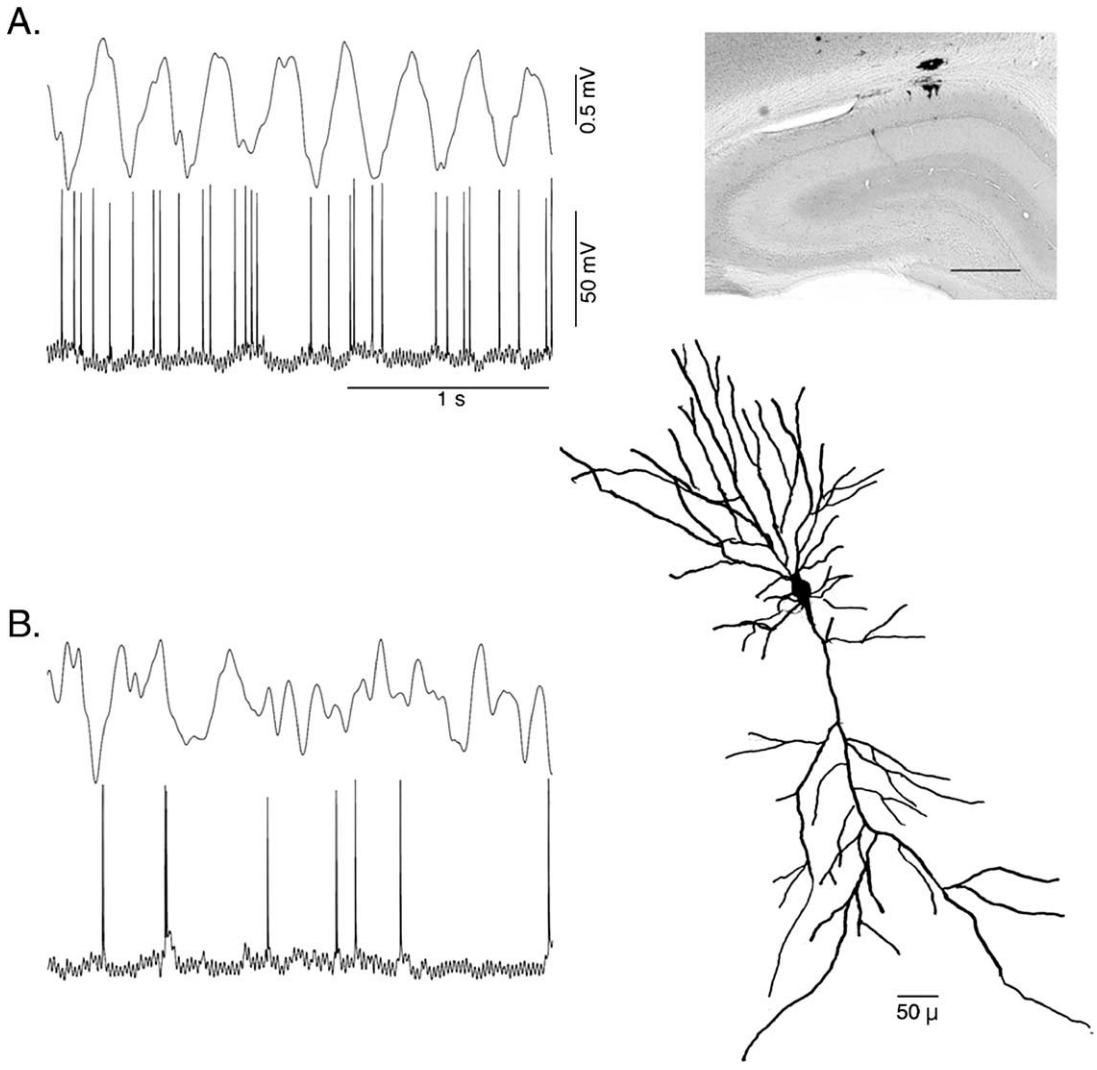

Fig. 4. (A) Relationship between spontaneously occurring hippocampal theta field activity and discharges of a CA1 pyramidal cell. Top: the hippocampal field activity recorded from the stratum moleculare of the dentate; bottom: the discharge pattern of a CA1 pyramidal cell (289) classified as a tonic theta-ON cell (positivity up in all traces). The cell discharged in an irregular pattern and MPOs were absent. (B) Relationship of the same cell to spontaneously occurring hippocampal LIA field activity. Note the overall lower discharge rate, irregular discharge pattern and lack of MPOs. Low power photomicrograph insert shows location of the cell in the CA1 pyramidal layer while the higher power magnification insert confirmed its identity as a CA1 pyramidal cell. Scale bar = 50 µ.

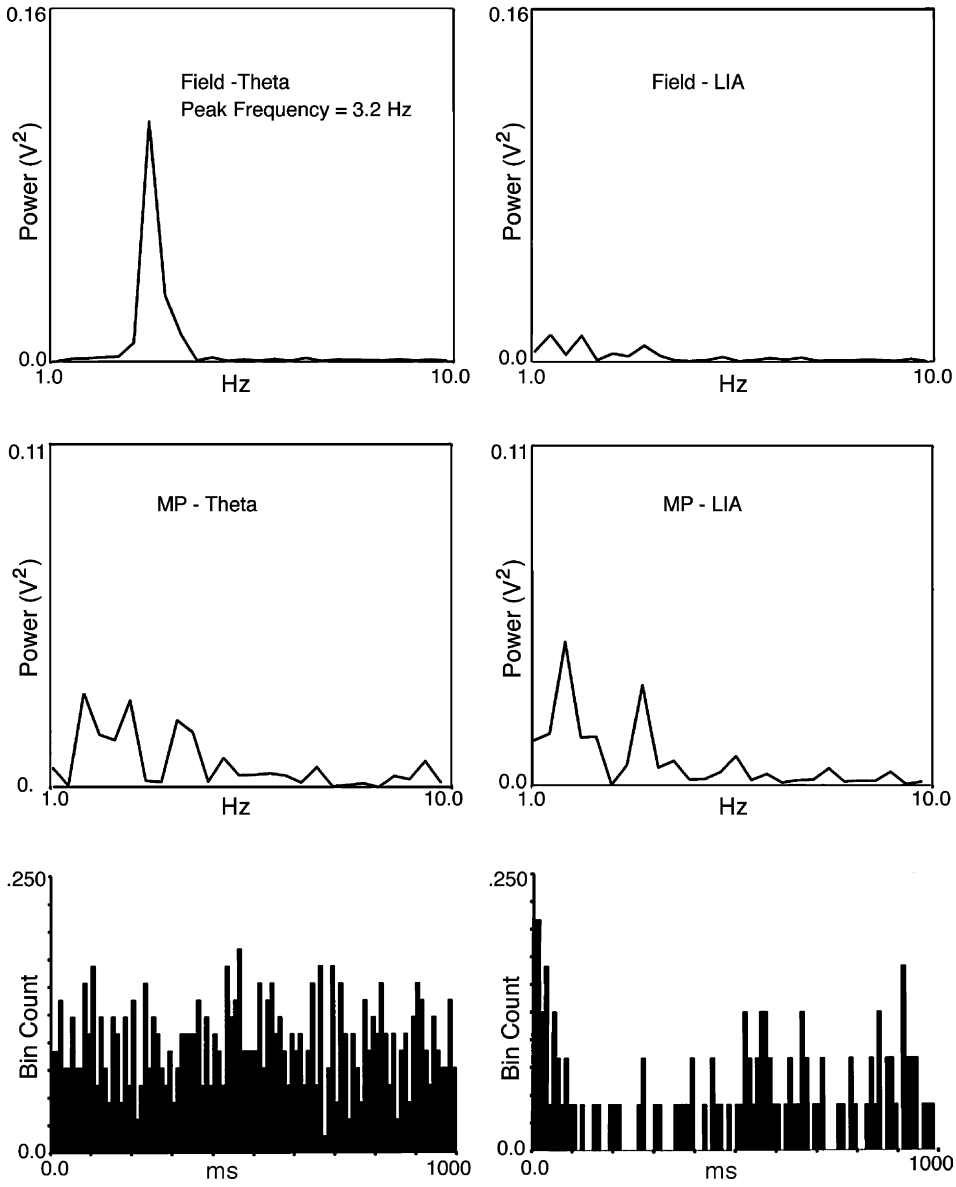

Fig. 5. Detailed analyses of the extracellular fields, intracellular membrane potentials and spike discharges of tonic theta-ON cell 289 during theta field activity (left-side panels) and LIA (right-side panels). Fast Fourier analysis of extracellular theta field activity (top left panel), fast Fourier analysis of MPOs during theta field activity (middle left panel) and autocorrelation histogram of irregular spike discharges during theta field activity (bottom left panel). Fast Fourier analysis of extracellular LIA field activity (top right panel), fast Fourier analysis of MPOs during theta field activity (middle right panel) and autocorrelation histogram of irregular spike discharges during LIA field activity (bottom right panel).

equivalent analyses for the LIA field conditions. The upper left panel is the FFT calculated for the extracellular theta field (mean frequency = 3.2 Hz), the middle left panel the FFT calculated for the MPOs (theta peak absent) and the lower left panel is the autocorrelation histogram of the spike train, indicating an irregular, non-rhythmic discharge pattern. The upper right panel is the FFT calculated for the LIA field condition (theta peak absent), the middle right panel the FFT calculated for the MPOs (theta peak absent) and the lower right panel is the autocorrelation histogram of the spike train, indicating an irregular, non-rhythmic discharge pattern and a lower discharge rate compared to that occurring during the theta field condition.

Non-related discharging CA1 pyramidal cells

Three out of 20 labeled CA1 pyramidal cells were classified as non-related, discharging CA1 pyramidal cells. These cells were classified as non-related since there were no significant differences in their discharge rates between the theta and LIA field conditions. Two of the non-related cells discharged in a simple spike pattern and one cell discharged with a complex spike pattern. Figs. 6A and B show recordings of a non-related CA1 pyramidal cell (cell 282) that discharged in an irregular simple spike pattern during both the spontaneous occurrence of HPC theta and LIA. The discharge rates accompanying the theta (mean

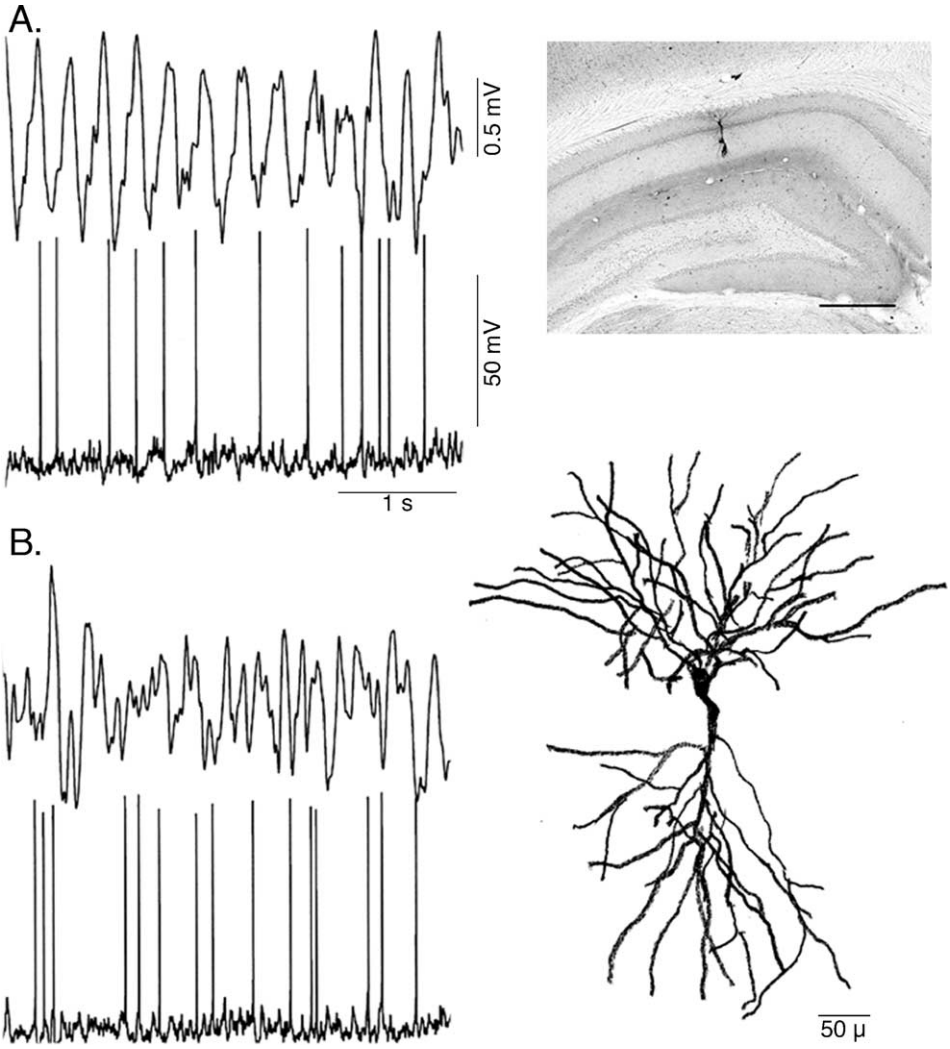

Fig. 6. (A) Relationships between spontaneously occurring hippocampal field activity and CA1 pyramidal cell discharges. Top: hippocampal field activity recorded from the stratum moleculare of the dentate; bottom: the discharge pattern of a CA1 pyramidal cell (282) classified as non-theta-related discharging (positivity up). The first part of the panel shows the irregular cell discharge pattern associated with LIA field activity, followed by a few seconds of theta field activity and then a return to LIA. Note the absence of MPOs. Low power photomicrograph insert shows location of the cell in the CA1 pyramidal layer while the higher power magnification insert confirmed its identity as a CA1 pyramidal cell. Scale bar = 50 μ.

discharge rate = 4.3 ± 0.39 Hz) and LIA (4.0 ± 0.39 Hz) conditions were not significantly different, and MPOs were absent during both conditions. The injection of Neurobiotin into cell 282 resulted in the labeling of one cell, shown in the low power photomicrograph insert to be located in the CA1 pyramidal layer and the higher magnification insert revealing its identity as a CA1 pyramidal cell. Fig. 7 presents the analyses carried out on cell 282 from Fig. 6. Left-side panels show analyses for the theta field conditions and right-side panels show the equivalent analyses for the LIA field conditions. The upper left panel is the FFT calculated for the extracellular theta field (mean frequency = 3.2 Hz), the middle left panel the FFT calculated for the MPOs (theta peak absent) and the lower left panel is the autocorrelation histogram of the spike train, indicating an irregular, non-rhythmic discharge pattern. The upper right panel is the FFT calculated for the LIA field condition (theta peak absent), the middle right panel the FFT calculated for the MPOs (theta peak absent) and the lower right panel is the autocorrelation histogram of the spike train, indicating an irregular, non-rhythmic discharge pattern. Fig. 8A shows an example of a recording of a non-related CA1 pyramidal cell (cell 291) that discharged in an irregular simple spike pattern during the spontaneous occurrence of HPC theta (mean discharge rate = 0.8 ± 0.14 Hz) and LIA (mean discharge rate = 1.1 ± 0.25 Hz), and in addition, would occasionally discharge in a complex spike pattern during LIA. Fig. 8B shows an example of a complex spike discharge with an expanded time base. The injection of Neurobiotin into cell 291 resulted in the labeling of three cells, shown in the low power photomicrograph insert to be located in the CA1 pyramidal layer and the higher magnification insert revealed their identity as CA1 pyramidal cells.

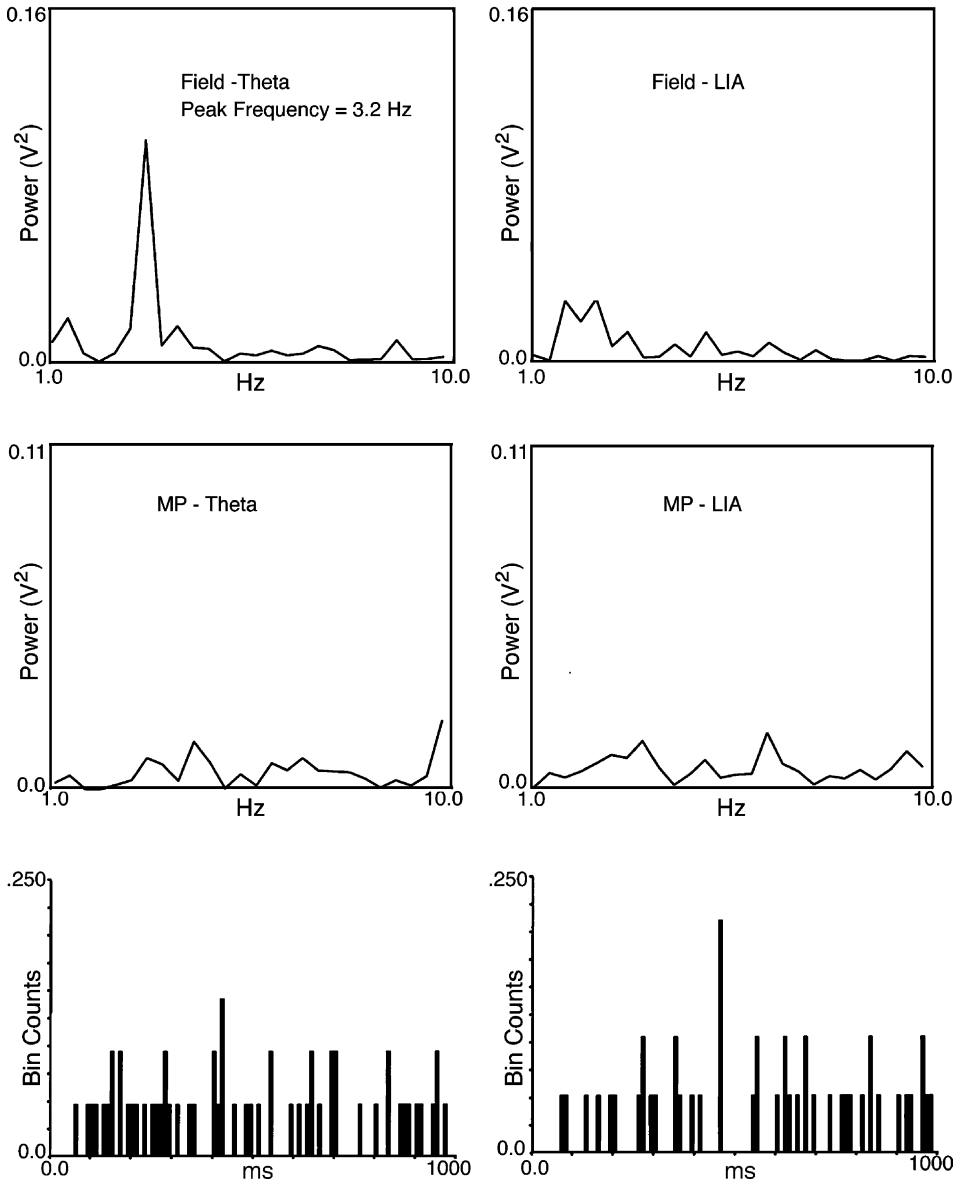

Fig. 7. Detailed analyses of the extracellular fields, intracellular membrane potentials and spike discharges of non-theta-related cell 282 during theta field activity (left-side panels) and LIA (right-side panels). Fast Fourier analysis of extracellular theta field activity (top left panel), fast Fourier analysis of MPOs during theta field activity (middle left panel) and autocorrelation histogram of irregular spike discharges during theta field activity (bottom left panel). Fast Fourier analysis of extracellular LIA field activity (top right panel), fast Fourier analysis of MPOs during theta field activity (middle right panel) and autocorrelation histogram of irregular spike discharges during LIA field activity (bottom right panel).

Non-related "silent" CA1 pyramidal cells

Six cells classified as non-related were totally silent during the spontaneous occurrence of both HPC theta and LIA. An example of a recording of one of these cells during both field conditions is shown in Fig. 9A. Fig. 9B shows the spike discharges elicited by a 100 pA depolarizing pulse. In addition to being silent, MPOs were absent during an average resting membrane potential of −71.5 mV. The injection of Neurobiotin into cell 281 resulted in the labeling of one cell, shown in the low power photomicrograph insert to be located in the CA1 pyramidal layer and the higher magnification insert revealing its identity as a CA1 pyramidal cell.

Theta and non-theta-related categories of identified CA3 pyramidal cells

A total of seven CA3 pyramidal cells were successfully recorded and as a result of multiple fills, 11 cells were labeled. These cells were classified according to the system of Colom and Bland (1987) as phasic theta-ON (n = 4) and non-related (n = 3). Non-related CA1 pyramidal cells were either of the discharging type (n = 2) or totally silent during

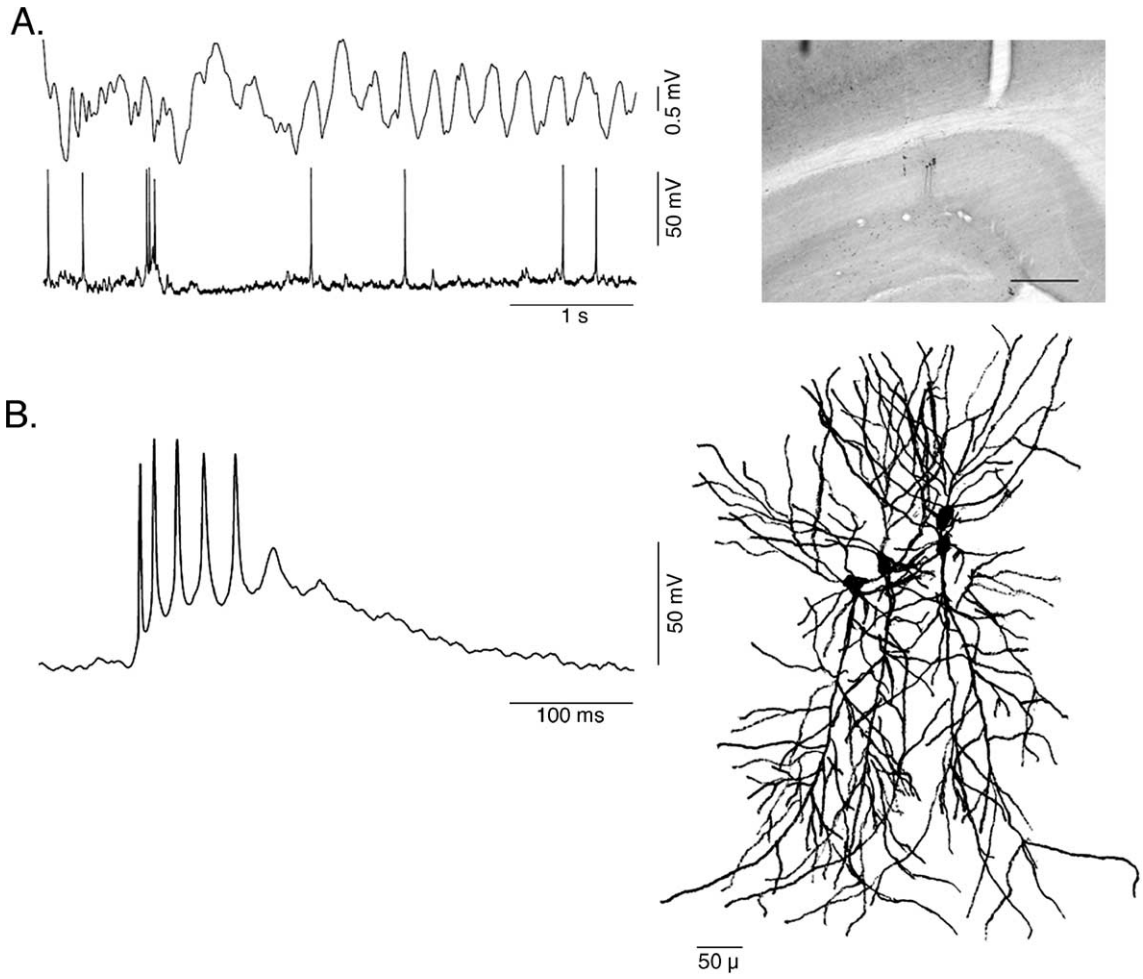

Fig. 8. (A) Relationships between spontaneously occurring hippocampal field activity and CA1 pyramidal cell discharges. Top: hippocampal field activity recorded from the stratum moleculare of the dentate; bottom: the discharge pattern of a CA1 pyramidal cell (291) classified as non-theta-related discharging (positivity up). The first half of the panel shows the irregular cell discharge pattern associated with LIA field activity and the second half shows the discharge pattern related to theta field activity. Note the occurrence of a complex spike discharge during LIA field activity and the complete absence of MPOs. (B) An expanded view of the complex spike discharge shown in panel A. Low power photomicrograph insert shows location of three labeled cells in the CA1 pyramidal layer while the higher power magnification insert confirmed that all three cells were CA1 pyramidal cells. Scale bar = 50 μ.

theta and LIA (n = 1). Data for all CA3 pyramidal cells are presented in Table 2.

CA3 pyramidal phasic theta-ON cells

Four out seven CA3 pyramidal cells were classified as phasic theta-ON cells. One recording resulted in the labeling of three pyramidal cells. Fig. 10 shows an example of one of these cell recordings (cell 309) during the spontaneous occurrence of either HPC theta (Fig. 10A) or LIA (Fig. 10B). During theta field activity, the cell membrane potential underwent a depolarizing shift of 5–10 mV and discharged 1–3 spikes (mean discharge rate = 6.9 ± 0.26 Hz) on the positive peak of well-developed intracellular MPOs (mean amplitude = 10.2 mV) and on the negative peak of the theta field activity (mean frequency = 3.5 Hz) recorded in the stratum oriens. During LIA, MPOs were absent and the cell discharged in an irregular, non-rhythmic pattern and exhibited an overall lower discharge rate (mean discharge rate = 3.5 ± 0.77 Hz) significantly different from the discharge rate during theta field activity (t = 3.78, P = 0.0016, $P < 0.05$). The injection of Neurobiotin into cell 309 resulted in the labeling of three cells, shown in the low power photomicrograph insert to be located in the CA3 pyramidal layer. The higher magnification insert revealed their identity as CA3 pyramidal cells although the fills were incomplete, resulting in poorly labeled apical dendrites.

Non-related discharging CA3 pyramidal cells

Two out of eight labeled CA3 pyramidal cells were classified as non-related, discharging CA3 pyramidal cells. These cells were classified as non-related since there were no significant differences in their discharge rates between the theta and LIA field conditions. These non-related cells discharged in a simple spike pattern. Fig. 11A shows an example of a recording of a non-related CA3 pyramidal cell (cell 308) during the spontaneous occurrence of HPC theta

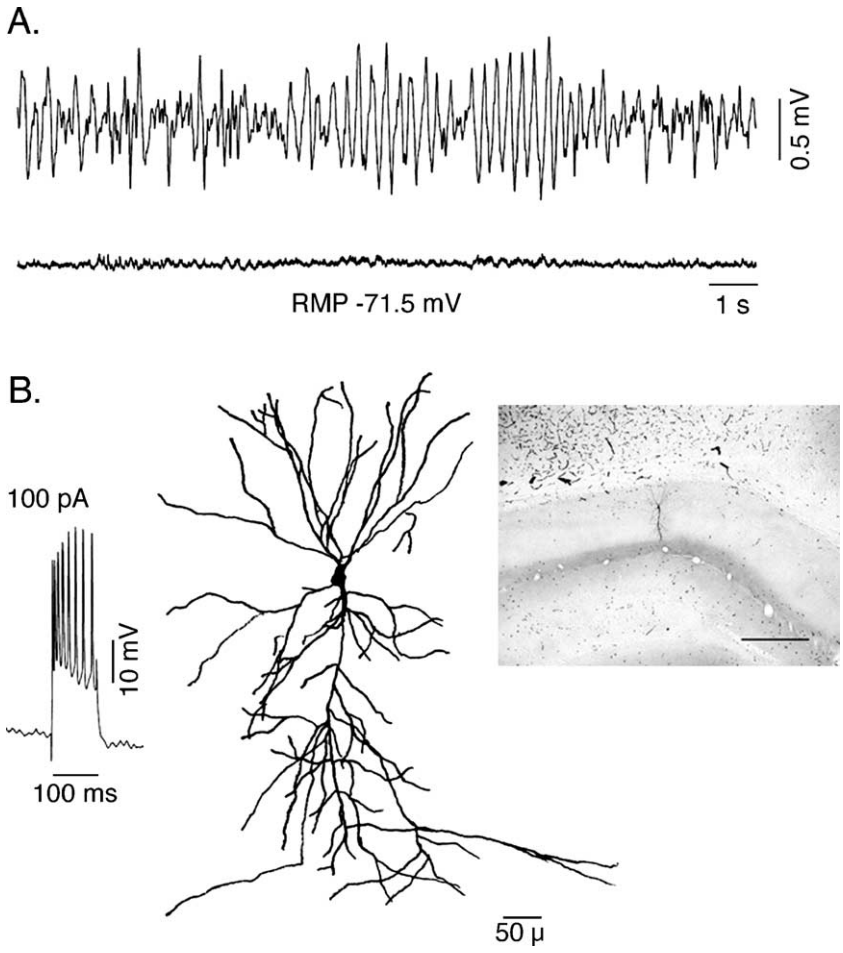

Fig. 9. (A) Relationships between spontaneously occurring hippocampal field activity and CA1 pyramidal cell discharges. Top: hippocampal field activity recorded from the stratum moleculare of the dentate; bottom: the membrane potential of a CA1 pyramidal cell (281) classified as non-theta-related "silent"(positivity up). The first half of the panel shows the occurrence of LIA field activity, followed by theta field activity and then LIA field activity. Note the complete absence of cell discharges and MPOs. (B) Cell discharges elicited by an intracellular depolarizing pulse. Low power photomicrograph insert shows location of the cell in the CA1 pyramidal layer while the higher power magnification insert confirmed its identity as a CA1 pyramidal cell. Scale bar = 50 μ.

and LIA (Fig. 11B). The discharge rates accompanying the theta (mean discharge rate = 9.67 ± 0.21 Hz) and LIA (9.9 ± 0.33 Hz) conditions were not significantly different, and MPOs were absent during both conditions. The injection of Neurobiotin into cell 308 resulted in the labeling of one cell, shown in the low power photomicrograph insert to be located in the CA3 pyramidal layer and the higher magnification insert revealing its identity as a CA3 pyramidal cell.

Non-related "silent" CA3 pyramidal cells

One cell classified as non-related was totally silent during the spontaneous occurrence of both HPC theta and

Table 2
CA3 pyramidal cell summary

Cell type and number	Cell class	Input resistance (MΩ)	Average membrane potential (mV)	Spike height (mV)	Average MPO amplitude (theta only) (mV)	Discharge rate—theta (mean ± SE)	Discharge rate—LIA (mean ± SE)
CA3 Pyr (253)	Phasic ON	28	60	55	6.2	7.3 ± 0.5*	3.2 ± 0.3
CA3 Pyr (301)	Phasic ON	25	62	63	7.5	4.4 ± 0.1*	2.0 ± 0.2
CA3 Pyr (302)	Phasic ON	29	58	60	8.7	7.6 ± 0.4*	3.4 ± 0.5
CA3 Pyr (309)	Phasic ON	30	60	50	10.2	6.9 ± 0.3*	3.5 ± 0.8
CA3 Pyr (275)	Silent	31	65	55	–	–	–
CA3 Pyr (285)	Discharging	27	61	70	–	1.8 ± 0.2	1.6 ± 0.2
CA3 Pyr (308)	Discharging	30	62	65	–	9.7 ± 0.2	9.9 ± 0.3

Asterisk indicates significant differences at $P < 0.05$.

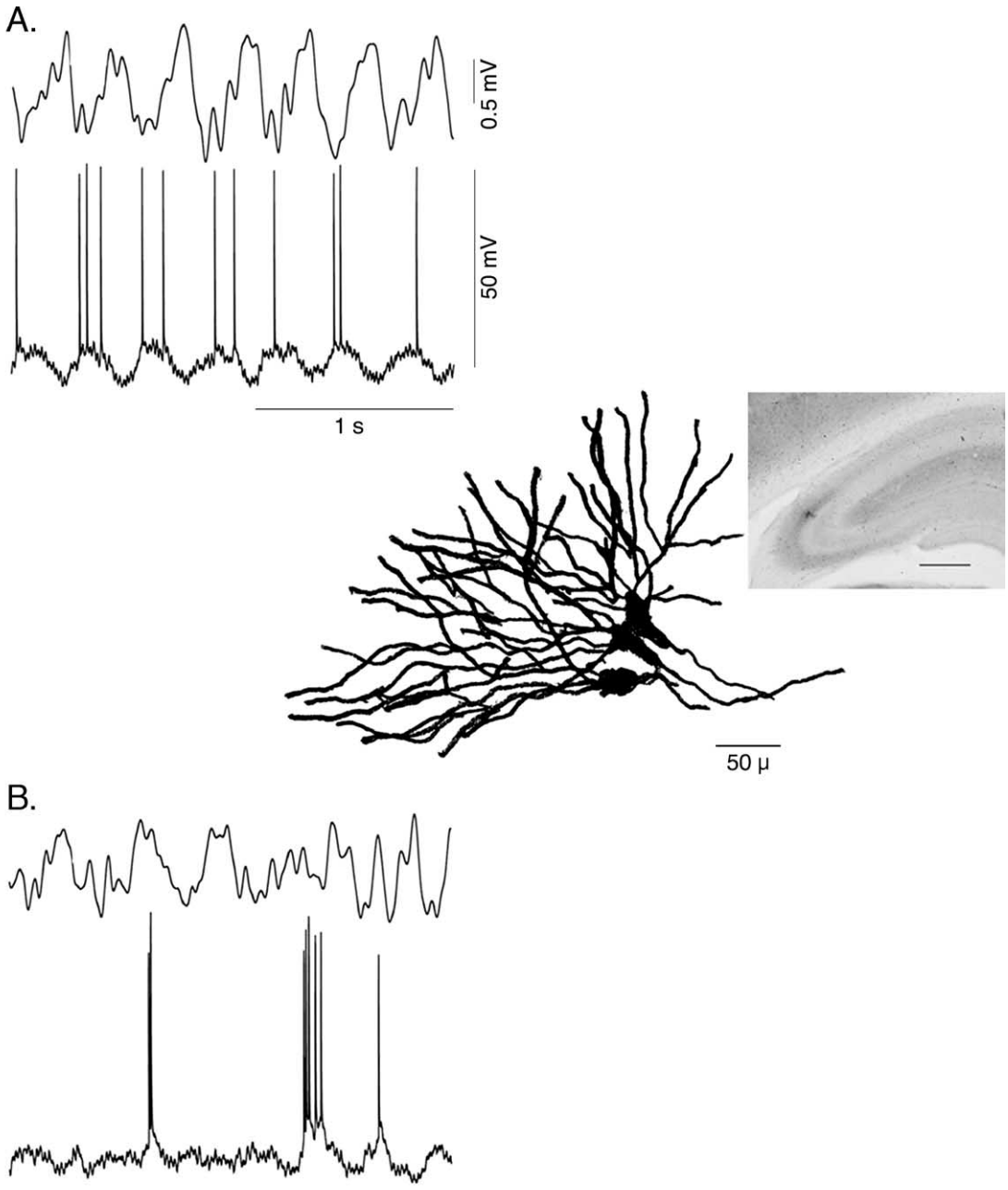

Fig. 10. (A) Relationship between spontaneously occurring hippocampal theta field activity and discharges of a CA3 pyramidal cell. Top: the hippocampal field activity recorded dorsal to the CA1 pyramidal cell layer in stratum oriens; bottom: the discharge pattern of a CA3 pyramidal cell (309) classified as a phasic theta-ON cell (positivity up in all traces). The cell discharged in a rhythmic pattern with 1–3 spikes riding on the positive phase of the MPOs and the negative phase of the extracellular theta field. (B) Relationship of the same cell to spontaneously occurring hippocampal LIA field activity. Note the overall lower discharge rate, irregular discharge pattern and lack of MPOs. Low power photomicrograph insert shows location of the cells in the CA3 pyramidal layer while the higher power magnification confirmed their identity as CA3 pyramidal cells. Apical dendrites were poorly labeled and not drawn. Scale bar = 50 µ.

LIA. An example of a recording of this cell during each field condition is shown in Fig. 12A. Fig. 12B shows the spike discharges elicited by a 200 pA depolarizing pulse. In addition to being silent, MPOs were absent during an average resting membrane potential of −65.4 mV. The injection of Neurobiotin into cell 275 resulted in the labeling of one cell, shown in the low power photomicrograph insert to be located in the CA3 pyramidal layer and the higher magnification insert revealed its identity as CA3 pyramidal cell.

Discussion

The major finding of the present study was the demonstration of functional heterogeneity among hippo-

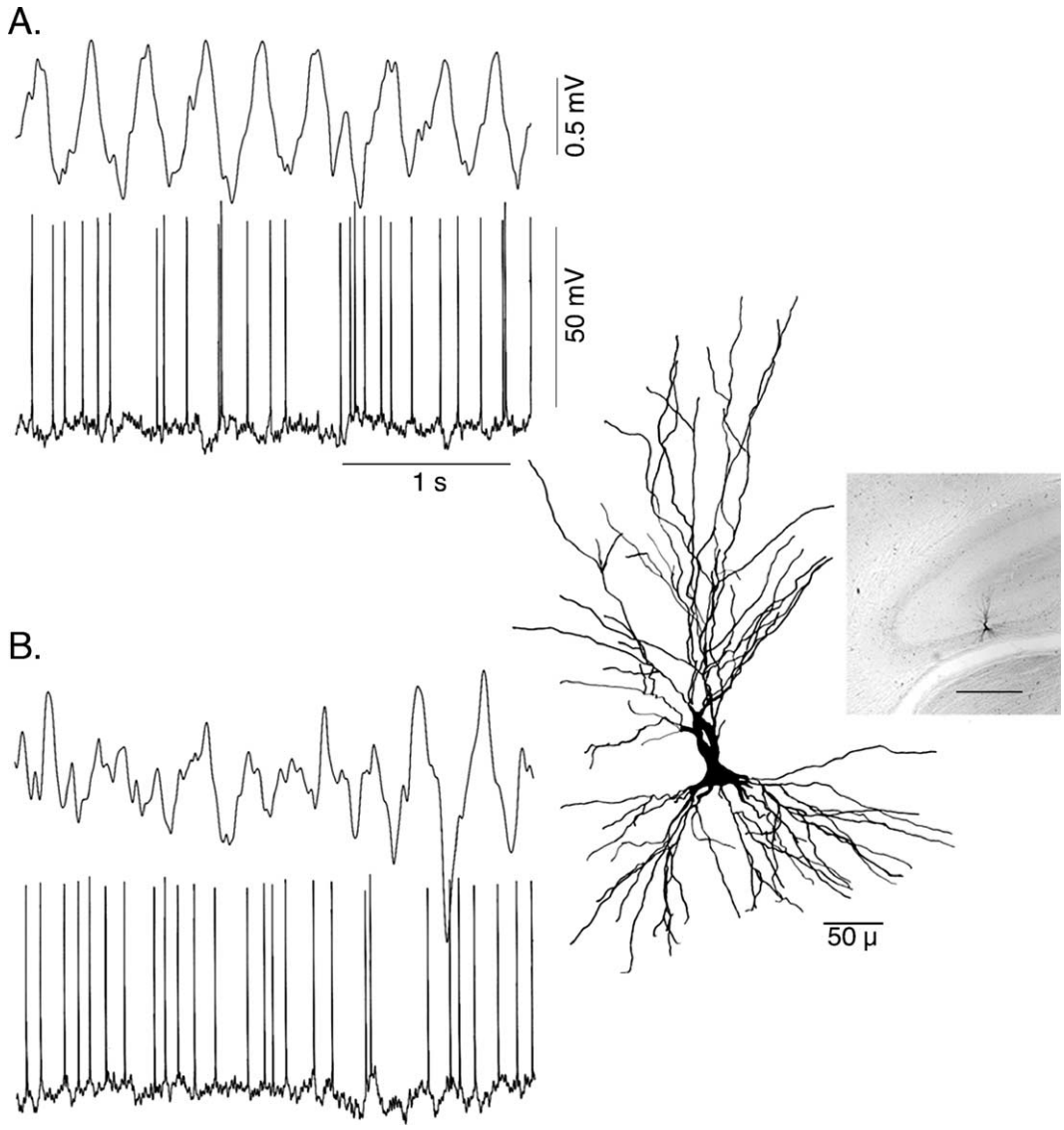

Fig. 11. (A) Relationship between spontaneously occurring hippocampal theta field activity and discharges of a CA3 pyramidal cell. Top: the hippocampal field activity recorded from the stratum moleculare of the dentate, bottom: the discharge pattern of a CA3 pyramidal cell (308) classified as a non-theta-related discharging cell (positivity up in all traces). The cell discharged in an irregular pattern and MPOs were absent. (B) Relationship of the same cell to spontaneously occurring hippocampal LIA field activity. Note the overall similar discharge rate, irregular discharge pattern and lack of MPOs during both field conditions. Low power photomicrograph insert shows location of the cell in the CA3 pyramidal layer while the higher power magnification insert confirmed its identity as a CA3 pyramidal cell. Scale bar = 50 μ.

campal pyramidal cells characterized in terms of their theta-related cell membrane potential and spike discharge properties. Subsets of CA1 theta-related pyramidal cells were phasic theta-ON cells, tonic theta-ON cells or non-theta-related cells. Non-theta-related CA1 pyramidal cells could discharge in a simple spike pattern while others could discharge in a complex spike pattern or remain totally silent, during the occurrence of both theta and LIA field conditions. Recordings of CA3 pyramidal cells revealed similar findings, with the exception that tonic theta-ON cells and complex spike firing non-related cells were not recorded. It is possible that these cell types existed but were not recorded as a result of fewer samples in the CA3 region.

Although direct anatomical identification was lacking, previous studies provided evidence for CA1 pyramidal cells being theta cells based on observations of rhythmic cell discharges and/or an "intracellular" theta rhythm (MPOs) (Fujita and Sato, 1964; Bland et al., 1988; Nunez et al., 1987, 1990; Leung and Yim, 1986, 1988, 1991; Fox, 1989; Konopacki et al., 1992). In the present study, nine-labeled CA1 cells were classified as phasic theta-ON cells while in a previous study, we reported the labeling of seven CA1 pyramidal cells meeting the criteria for classification as phasic theta-ON cells (Bland et al., 2002). The evidence is thus overwhelmingly in favor of a subset of CA1 pyramidal cells being theta cells (phasic theta-ON cells in our terminology). The present study also demonstrated that

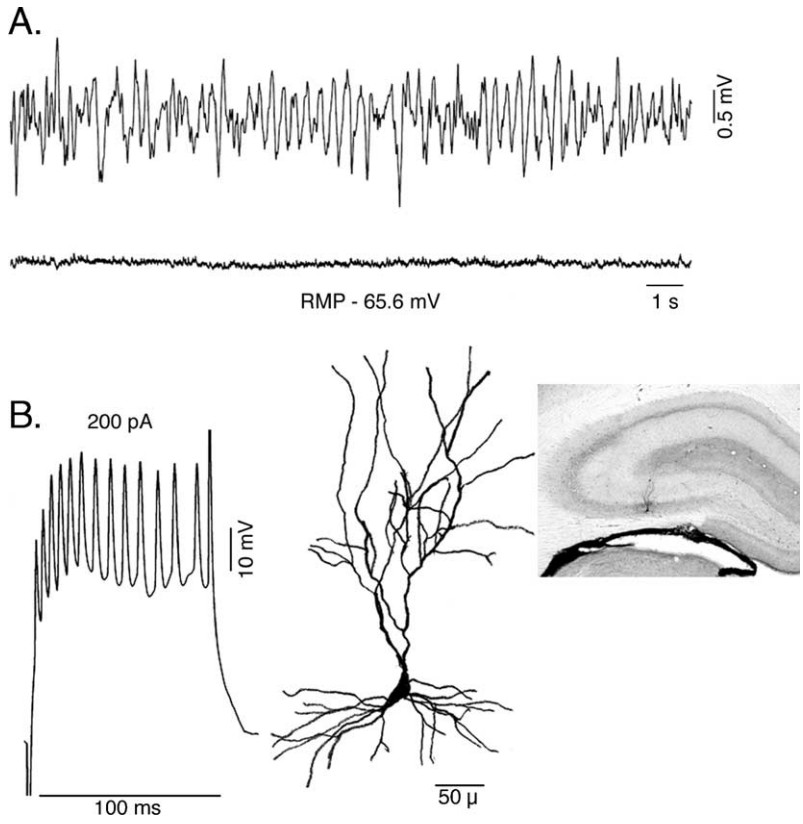

Fig. 12. (A) Relationships between spontaneously occurring hippocampal field activity and CA3 pyramidal cell discharges. Top: hippocampal field activity recorded from the stratum moleculare of the dentate; bottom: the membrane potential of a CA3 pyramidal cell (275) classified as non-theta-related "silent"(positivity up). The first half of the panel shows the occurrence of LIA field activity, followed by theta field activity alternating with LIA field activity. Note the complete absence of cell discharges and MPOs. (B) Cell discharges elicited by an intracellular depolarizing pulse. Low power photomicrograph insert shows location of the cell in the CA3 pyramidal layer while the higher power magnification insert confirmed its identity as a CA3 pyramidal cell. Scale bar = 50 µ.

the same conclusion might be applied to a subset of CA3 pyramidal cells. CA1 and CA3 pyramidal phasic theta-ON cells always exhibited MPOs during theta field activity but never during LIA field activity. At the onset of theta, MPOs occurred as the membrane potential underwent a 5–10 mV depolarizing shift, with rhythmic spike discharges occurring on the positive phase of the MPOs and phase locked to the simultaneously occurring extracellular theta waves. Bland et al. (2002), Komondi et al. (1998), Soltesz and Deschenes (1993) and Ylinen et al. (1995) demonstrated that the amplitudes of MPOs in CA1 pyramidal cells were voltage-dependent while their frequencies were voltage-independent. Furthermore, Bland et al. (2002) showed that the amplitude of MPOs in CA1 pyramidal cells played a critical role in determining both spike rhythmicity and the number of spike discharges occurring per oscillation, during theta field activity. Strata (1998) demonstrated that CA3 pyramidal cells recorded from juvenile and adult slices of hippocampus were endowed with intrinsic properties that allowed the generation of steady oscillatory activity (MPOs). The frequency of this rhythmic ongoing process was highly sensitive to the level of the membrane potential, reaching values in the theta range, up to 6 Hz, for more depolarized values of membrane potential. Membrane potential oscillations were unmasked by loading pyramidal neurons with intracellular cesium, were sodium-independent and were generated by the sequential activation of calcium and potassium conductances. Strata (1998) also demonstrated that like theta field activity, regularly occurring membrane potential oscillations could be detected since postnatal day 10 and their frequency increased with age during the first 2 weeks. These latter findings supported those of the development of theta field activity reported by LeBlanc and Bland (1979) in the freely moving rat and Konopacki et al. (1988) in hippocampal slices. It is of some interest that, in the Strata (1998) study, MPO frequencies were sensitive to membrane potential values, an observation also reported by Leung and Yu (1998). The two former studies were carried out in the in vivo slice preparation whereas Bland et al. (2002), Komondi et al. (1998), Soltesz and Deschenes (1993) and Ylinen et al. (1995) all reported that the frequencies of MPOs were voltage-independent and MPO amplitudes were voltage-dependent, using in vivo preparations. This difference between the in vitro and in vivo studies may be due to the absence of septal GABA-ergic projections in the slice preparations (Bland and

Colom, 1993). Regardless, the demonstration of intrinsically generated MPOs in hippocampal pyramidal cells supports the model of theta generation proposed by Bland and Colom (1993). These authors proposed that synaptic inputs to hippocampal pyramidal cells served to achieve three purposes: (1) synchronize the MPOs of these cells and the resulting synchronization is manifested as extracellular theta band field oscillations; (2) synaptic inputs, in addition to synchronizing MPOs, serve to drive the MPOs at different frequencies by providing varying levels of tonic depolarization; (3) synaptic inputs serve to reset the ongoing MPO frequencies.

As discussed above, there is good agreement on the voltage dependence of MPOs in CA1 pyramidal cells between the Bland et al. (2002) paper and the papers by Komondi et al. (1998), Soltesz and Deschenes (1993) and Ylinen et al. (1995), using in vivo preparations. In addition, both the Bland et al. and Ylinen et al. studies reported that the application of varying levels of depolarizing intracellular currents during the occurrence of LIA (non-theta) activity failed to induce MPOs. There were, however, some discrepancies on several points. Soltesz and Deschenes (1993) and Ylinen et al. (1995) reported an approximate 180° phase shift in CA1 cells that were hyperpolarized from −65 to −85 mV while Bland et al. (2002) did not see any phase shifting. On the contrary, these authors demonstrated that the injection of hyperpolarizing and depolarizing constant current pulses resulted in an inverted U-shaped function. Soltesz and Deschenes (1993) and Ylinen et al. (1995), both selected low firing (<1 and 2 HZ, respectively) pyramidal cells for analysis, whereas in the Bland et al. (2002) study, the cells discharged between 10 and 12 Hz. The demonstrated heterogeneity of CA1 pyramidal cells in the present study may thus explain some of the difference between the studies. A major discrepancy between the Komondi et al. (1998) and Ylinen et al. (1995) studies and the Bland et al. (2002) study concerns the membrane potential changes and cell discharge patterns during theta band field oscillations. The Bland et al. paper, the Konopacki et al. (1992) paper and the current work demonstrated that a large subset of CA1 pyramidal cells may be classified as theta-ON cells, with the membrane potential undergoing a depolarizing shift at the onset of theta field activity accompanied by a number of rhythmical spike discharges riding on the depolarizing phase of the MPOs. Ylinen et al. (1995) stated, “In summary, the intracellular experiments favor the view that most pyramidal cells during theta activity are hyperpolarized.” Komondi et al. (1998) reported that the onset of theta overlaps in time with somatic hyperpolarization of CA1 pyramidal cells and as a result, most pyramidal cells are either silent or discharge with single spikes on the negative portion of local field theta, supporting the results of Ylinen et al. (1995). Since the CA1 pyramidal cells reported in their studies did exhibit MPOs, the results of the present paper fail to address this major discrepancy.

CA1 pyramidal cells also form a subset of tonic theta-ON cells. Cells in this category significantly increased their discharge rates during theta field activity compared to LIA, but did not display rhythmic discharge patterns or MPOs during theta. CA1 and CA3 pyramidal cells also formed subsets of non-theta-related cell populations. The discharges of such identified cells ranged from irregular simple spike patterns and complex spike patterns to total silence, during the spontaneous occurrence of hippocampal field activities.

Taken together with the discussion above, the findings of the present paper clearly demonstrate that the identification of a hippocampal cell as pyramidal does not imply functional homogeneity. Fox and Ranck (1975), on the basis of studying hippocampal cells recorded extracellulary in unrestrained rats, concluded that the class of projection cells and the class of non-theta cells had a very large overlap, and the class of interneurons and the class of theta cells had a very large overlap. These findings have led to the predominant view in the theta literature that hippocampal pyramidal cells are complex spike cells, not theta cells and indeed, that hippocampal interneurons are theta cells. The present paper demonstrated that contrary to this widely held view, subsets of hippocampal pyramidal cells could be either phasic or tonic theta-ON cells, as well as several types of non-theta-related cells. A major caveat of the present work was the use of urethane-anesthetized preparations, while the Fox and Ranck work used freely moving animals. The use of urethane results in a bias towards predominantly type 2 theta activity (cholinergically-mediated theta; see Bland, 1986). We do, however, consider it unlikely that cells will change their theta-related classifications revealed under urethane in any dramatic manner in the freely moving condition, that is, “on” cells becoming “off” cells and vice-versa for example. The differences are more likely to be reflected in changes in discharge rates related to behavior. For example, theta cells in freely moving rabbits discharged rhythmically but at lower rate during immobile sensory processing conditions (Type 2 theta) compared to walking and hopping (Type 1 plus type 2 theta condition), even when extracellular theta field frequencies were identical (Bland et al., 1983). While the unequivocal resolution of the differences between the present study and the study by Fox and Ranck will likely be a long time coming, the results of the present work should still be given serious consideration when attempting explanations and/or modeling of the neural circuitry underlying the generation of theta-band oscillation and synchrony.

Bland and Colom’s (1993) proposal that hippocampal theta-OFF cells were comprised of a subset of interneurons was also recently supported by the findings of Bland et al. (2002) who reported recording nine cells localized to the CA1 pyramidal cell layer (one of which was labeled), meeting the criteria for theta-OFF cells. Further indirect support for this proposal is provided by the fact that, of 20 recordings in identified CA1 pyramidal cells in the present

study, not one cell met the criteria for being classified as a theta-OFF cell. The present study did not provide any direct evidence to resolve the differences in the findings for basket cells between the Bland et al. (2002) study and the Ylinen et al. (1995) study. The latter authors provided evidence for 3 labeled basket cells (and one non-labeled cell) showing the characteristics of a theta cell (theta-ON), that is, well developed MPOs with rhythmic spike discharges occurring on the positive phase. Bland et al. provided evidence that one labeled basket cell (and eight non-labeled cells) in the CA1 pyramidal layer met their criteria for phasic theta-OFF cells. This included well-developed MPOs during theta superimposed on a hyperpolarizing shift of the membrane potential, with a complete inhibition of cell discharges at higher theta frequencies. When theta frequency decreased, just prior to the transition to LIA, the membrane potential depolarized to the point where a few rhythmic cell discharges were superimposed on the MPOs. Upon the transition to LIA, cell discharge rates increased and the pattern became irregular. Bland et al. (2002) also demonstrated that the MPOs in CA1 pyramidal layer basket cells underwent an approximate 180° phase reversal when the membrane potential was depolarized above −65 mV. This finding supported the conclusion that MPOs in basket cells were synaptically mediated and that chloride-dependent IPSPs played a role in their generation. The low numbers of labeled basket cells in both studies leave open the possibility that there are subsets of these cells equivalent to those of pyramidal cells, in terms of their theta-related properties.

Bland and Colom (1993) suggested that ephaptic properties and gap junctions might also contribute to the generation of theta-band oscillation and synchrony. Konopacki et al. (2004) provided evidence for the involvement of gap junctions in the generation of carbachol-induced theta in hippocampal slices. These authors demonstrated that the treatment of hippocampal slices with the gap junction blockers carbenoxolone and quinine blocked cholinergically induced theta field activity and related cell discharges. The multi-labeling of cells with Neurobiotin, while not definitive evidence for gap junctions, does provide support for their involvement in the generation of theta. Bland et al. (2002) reported an incidence of 57% for multi-labeled cells, while the incidence in the present study was 33%.

In summary, the results of the present paper indicate that the generation of theta field activity is very complicated and caution should be exercised in drawing conclusions based on cellular morphology alone.

Acknowledgment

Grant sponsor: Natural Sciences and Engineering Research Council of Canada; Grant number: A9935 to B. H. Bland and A217322 to R. Dyck.

References

Bland, B.H., 1986. The physiology and pharmacology of hippocampal formation theta rhythms. Prog. Neurobiol. 26, 1–54.

Bland, B.H., 2000. The medial septum: node of the ascending brainstem hippocampal synchronizing pathways. In: Numan, R. (Ed.), The Behavioral Neuroscience of the Septal Region. Springer Verlag, New York, NY, pp. 115–145.

Bland, B.H., Colom, L.V., 1993. Extrinsic and intrinsic properties underlying oscillation and synchrony in limbic cortex. Prog. Neurobiol. 41, 157–208.

Bland, B.H., Konopacki, J., 2000. Intracellular recording and staining in the acute in vivo rat using sharp electrodes. Kopf Carrier 52, 1–6.

Bland, B.H., Oddie, S.D., 1998. Anatomical, electrophysiological and pharmacological studies of ascending brainstem hippocampal synchronizing pathways. Neurosci. Biobehav. Rev. 22, 259–273.

Bland, B.H., Oddie, S.D., 2001. Theta band oscillation and synchrony in the hippocampal formation and related structures: the case for its role in sensorimotor integration. Behav. Brain Res. 127, 119–136.

Bland, B.H., Seto, M.G., Rowntree, C.I., 1983. The relation of multiple hippocampal theta cell discharge rates to slow wave theta frequency. Physiol. Behav. 31, 11–117.

Bland, B.H., Colom, L.V., Konopacki, J., Roth, S.H., 1988. Intracellular records of carbachol-induced theta rhythm in hippocampal slices. Brain Res. 474, 364–368.

Bland, B.H., Konopacki, J., Dyck, R., 2002. Relationship between membrane potential oscillations and rhythmic discharges in identified hippocampal theta-related cells J. Neurophysiology 88, 3046–3066.

Buzsaki, G., 2002. Theta oscillations in the hippocampus. Neuron 33, 325–340.

Colom, L.V., Bland, B.H., 1987. State-dependent spike train dynamics of hippocampal formation neurons: evidence for theta-ON and theta-OFF cells. Brain Res. 422, 277–286.

Fox, S.E., 1989. Membrane potential and impedance changes in hippocampal pyramidal cells during theta rhythm. Exp. Brain Res. 77, 283–294.

Fox, S.E., Ranck, J.B., 1975. Localization and anatomical identification of theta and complex spike cells in dorsal hippocampal formation of rats. Exp. Neurol. 49, 229–313.

Fujita, Y., Sato, T., 1964. Intracellular records from hippocampal pyramidal cells in rabbits during theta rhythm activity. J. Neurophysiol. 27, 1011–1025.

Kita, H., Armstrong, W., 1991. A biotin-containing compound N-2 (2-aminoethyl) biotinamide for intracellular labeling and neuronal tracing studies. Comparison with biocytin. J. Neurosci. Methods 37, 141–150.

Komondi, A., Laszlo, A., Wang, X-J., Buzsaki, G., 1998. Theta oscillations in somata and dendrites of hippocampal pyramidal cells in vivo: activity-dependent phase-precession of action potentials. Hippocampus 8, 244–261.

Konopacki, J., Bland, B.H., Roth, S.H., 1988. The development of carbachol-induced EEG theta examined in hippocampal formation slices. Dev. Brain Res. 38, 229–232.

Konopacki, J., Bland, B.H., Colom, L.V., Oddie, S.D., 1992. In vivo intracellular correlates of hippocampal formation theta-on and theta-off cells. Brain Res. 586, 247–255.

Konopacki, J., Bland, B.H., Dyck, R.D., 2003. Intracellular recording and labeling of neurons in midline structures of the rat brain in vivo using sharp electrodes. J. Neurosci. Meth. 127, 85–93.

Konopacki, J., Kowalczyk, T., Golebiewski, H., 2004. Electrical coupling underlies theta oscillations recorded in hippocampal formation slices. Brain Res. 1019, 270–274.

LeBlanc, O., Bland, B.H., 1979. Developmental aspects of hippocampal electrical activity and motor behavior I the rat. Exp. Neurol. 66, 220–237.

Leung, L.-W.S., Yim, C.-Y., 1986. Intracellular records of theta rhythm in hippocampal CA1 cells of the rat. Brain Res. 367, 323–327.

Leung, L.-W.S., Yim, C.-Y., 1988. Membrane potential oscillations in hippocampal neurons in vitro induced by carbachol or depolarizing currents. Neurosci. Res. Commun. 2, 159–167.

Leung, L.-W.S., Yim, C.-Y., 1991. Intrinsic membrane potential oscillations in hippocampal neurons in vitro. Brain Res. 553, 261–274.

Leung, L.-W.S., Yu, H.W., 1998. Theta frequency resonance in hippocampal CA1 neurons in vivo demonstrated by sinusoidal current injection. J. Neurophysiol. 79, 1592–1596.

Leung, L.-W.S., Lopes Da Silva, F.H., Waddman, W.J., 1982. Spectral characteristics of the hippocampal EEG in freely moving rat. Electroencephalogr. Clin. Neurophysiol. 54, 203–219.

Nunez, A., Garcia-Austt, E., Buno Jr., W., 1987. Intracellular theta rhythm generation in identified hippocampal pyramids. Brain Res. 416, 289–300.

Nunez, A., Garcia-Austt, E., Buno Jr., W., 1990. Synaptic contributions to theta rhythm genesis in rat CA1–CA3 hippocampal pyramidal neurons in vivo. Brain Res. 533, 176–179.

Soltesz, I., Deschenes, M., 1993. Low and high frequency membrane potential oscillations during theta activity in CA1 and CA3 pyramidal neurons of the rat under ketamine-xylazine anesthesia. J. Neurophysiol. 70, 97–116.

Strata, F., 1998. Intrinsic oscillations in CA3 hippocampal pyramids: physiological relevance to theta rhythm generation. Hippocampus 8, 666–679.

Vertes, R.P., Kocsis, B., 1997. Brainstem–diencephalo–septohippocampal systems controlling the theta rhythm of the hippocampus. Neuroscience 81, 893–926.

Vertes, R.P., Hoover, W.B., Di Prisco, G.V., 2004. Theta rhythm of the hippocampus: subcortical control and functional significance. Behav. Cogn. Neurosci. Rev. 3, 173–200.

Ylinen, A., Solstez, I., Bragin, A., Penttonen, M., Sik, A., Buzsaki, G., 1995. Intracellular correlates of hippocampal theta rhythm in identified pyramidal cells, granule cells, and basket cells. Hippocampus 5, 78–90.